JOURNAL OF MATERIALS SCIENCE 16 (1981) 489–494

The equilibrium defect structure of iron-doped MgO in the range 600–1200° C

T. A. YAGER, W. D. KINGERY
Department of Materials Science and Engineering, Massachusetts Institute of Technology, Cambridge, Massachusetts 02139, USA

High-temperature electron paramagnetic resonance (EPR) spectroscopy with a CO_2 laser heat source was used to study the 600 to 1200° C point defects and precipitates in MgO doped with up to 4300 ppm Fe. Mass action relations incorporating Debye–Hückel activity coefficient corrections were developed to describe $Fe_{Mg}^{\cdot}$–V_{Mg}'' association and magnesioferrite precipitation.

1. Introduction

Trivalent iron forms substitutional solid solutions in MgO with its effective positive charge compensated by the negative magnesium ion vacancies. Using Kröger–Vink notation, the solution of trivalent iron in MgO can be written

$$Fe_2O_3 \xrightarrow{MgO} 2Fe_{Mg}^{\cdot} + V_{Mg}'' + 3O_O^x$$

Coulombic attraction between $Fe_{Mg}^{\cdot}$ and V_{Mg}'' results in association to form a negatively charged dimer according to the reaction

$$Fe_{Mg}^{\cdot} + V_{Mg}'' = (Fe_{Mg}^{\cdot} - V_{Mg}'')'. \quad (1)$$

Depending on the location of the vacancy, a dimer may be oriented in either the ⟨1 0 0⟩ (termed D⟨1 0 0⟩) or the ⟨1 1 0⟩ (termed D⟨1 1 0⟩) crystallographic direction. Additional association may occur due to the coulombic attraction of a dimer and another iron ion to form a neutral trimer

$$(Fe_{Mg}^{\cdot} - V_{Mg}'')' + Fe_{Mg}^{\cdot} = (Fe_{Mg}^{\cdot} - V_{Mg}'' - Fe_{Mg}^{\cdot})^x. \quad (2)$$

Linear trimers can form along ⟨1 0 0⟩ or ⟨1 1 0⟩ directions, and several non-linear trimers may exist [1, 2].

Phase separation occurs to form magnesioferrite spinel precipitates

$$Mg_{Mg}^x + 2Fe_{Mg}^{\cdot} + V_{Mg}'' + 4O_O^x = MgFe_2O_{4(ppt)}. \quad (3)$$

Since dimers and trimers are present during phase separation, the actual reaction process is some unknown combination of Equations 1, 2 and 3 [1, 2].

Association and clustering processes were found to occur sufficiently rapidly that local high-temperature structures were not maintained in the room-temperature material after quenching [3]. Thus the defect structure of quenched MgO does not correspond to the equilibrium high temperature structure. The present study applies high-temperature electron paramagnetic resonance (EPR) spectroscopy to the analysis of the equilibrium defect structure of Fe^{3+}-doped MgO in the temperature range 600 to 1200° C. This technique eliminates the quench problem by permitting simultaneous measurement of different defect concentrations *in situ*. In addition, the ability of EPR spectroscopy to detect low concentrations of ferrimagnetic precipitates has provided a means of extending phase equilibria measurements to low solute levels.

2. Experimental procedure

2.1. Association measurements

Single crystals of 4N (99.99% pure) MgO doped in the melt with 310, 2300 and 4300 ppm iron were obtained from W. and C. Spicer, Ltd., Cheltenham, England. The samples were cleaved along {1 0 0} planes to produce sample dimensions of 4.8 mm × 4.8 mm × 1 mm. To fully oxidize and homogenize all solutes, the sample was slowly heated to 1600° C in flowing O_2, lowered to 1100° C for 24 h and quenched into liquid nitrogen.

0022–2461/81/020489–06$02.60/0

High-temperature EPR spectroscopy with a CO_2 laser heat source [4] was used to monitor defect concentrations at temperatures up to 1200° C. The sample was positioned in the spectrometer with the magnetic field parallel to the [1 0 0] direction, and initially heated for 0.5 h at 1200° C to allow the sample, microwave cavity and laser to reach a stable thermal equilibrium. Then the temperature was lowered at a rate equal to 100° C h^{-1}, and the EPR spectra were recorded at 25° C intervals. Calculations indicated that between 850 and 1200° C this rate of temperature change was sufficiently rapid to prevent a change in the ratio Fe^{3+}/Fe^{2+} yet sufficiently slow to allow equilibrium association to occur. From 700 to 850° C the temperature was lowered at a rate of 50° C h^{-1}, and below 700° C at 25° C h^{-1}. Samples were first tested with decreasing temperature and then with increasing temperature.

2.2. Phase equilibria measurements

On cooling to room temperature the EPR spectrum was almost completely masked by a very broad peak centred near $g = 2$. This peak has been previously reported [5, 6] and related to ferrimagnetic precipitate resonance. The broad peak was often accompanied by an orange colouration of the sample, and both were removed by a short annealing period above 1000° C followed by quenching. That is, quenching was sufficiently rapid to prevent precipitation during the quench.

To confirm the identification of this broad resonance the temperature dependence of the peak intensity was studied. The intensity was found to decay monotonically as the temperature increased, and was completely absent at 210° C. This corresponded to the Curie temperature of 217° C measured by Wirtz and Fine [7] on magnesioferrite particles precipitated from MgO containing approximately 1% Fe.

Samples of 310, 2300 and 4300 ppm Fe were tested in this manner to detect phase separation. Samples were first oxidized as described above and heat treatments were conducted in flowing O_2 near the temperature of phase separation. Following each heat treatment, the sample was quenched into liquid nitrogen and the room-temperature EPR spectra recorded. By detecting the presence or absence of the broad peak and repeating the procedure, the temperature interval was narrowed. It was found that a 5° C change in temperature would either produce or remove the peak. The times of the anneals were adjusted for the temperature of interest: above 950° C, 25 h anneals were used; from 850 to 950° C, 72 h anneals were used; and from 750 to 850° C, one week anneals were used. Following this investigation, the crystals were analysed for Fe by quantitative atomic absorption spectroscopy.*

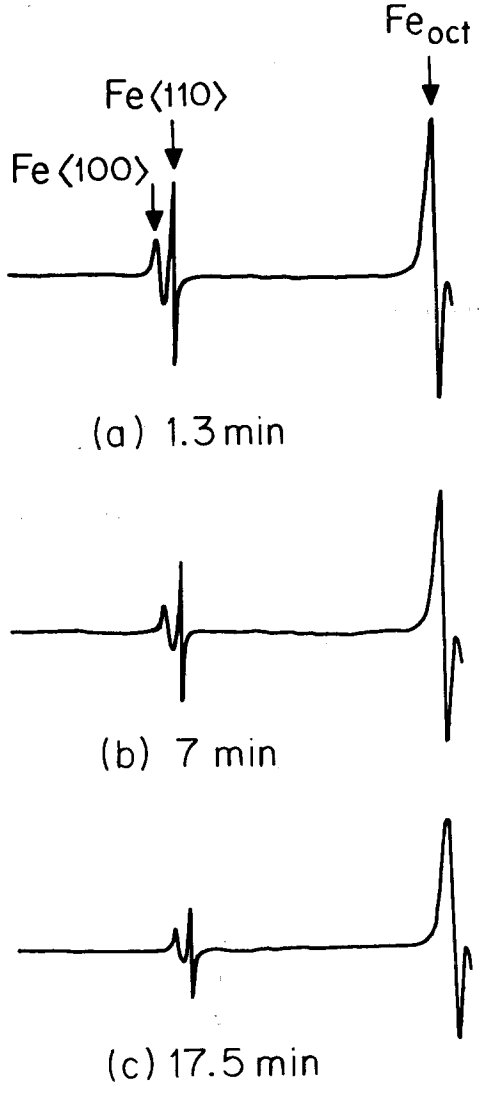

Figure 1 EPR spectra of MgO containing 4300 ppm Fe at three different temperatures.

3. Results and analysis

3.1. The spectra

EPR spectra of MgO containing 4300 ppm Fe at 600, 900 and 1200° C are shown in Fig. 1. Peaks have been labelled Fe⟨1 0 0⟩, Fe⟨1 1 0⟩ and Fe_{oct}

*Analysis performed by W. Carrera, MIT.

attributed to $Fe_{Mg}^{\cdot} - V_{Mg}''$ associates oriented in the ⟨1 0 0⟩ direction [8], the ⟨1 1 0⟩ direction [9] and an unassociated $Fe_{Mg}^{\cdot}$ [10]. The Fe_{oct} peak is the low magnetic field part of a well-known quintet of peaks attributed to Fe^{3+} in an octahedral site [10]. Rotation of the magnetic field around the crystal identified the Fe⟨1 0 0⟩ and Fe⟨1 1 0⟩ spectral peaks as due to tetragonal [8] and orthorhombic [9] defect centres. Explicit identification of the defect producing the crystal field perturbation is not possible from the EPR data alone, but since the concentration of monovalent impurities is much lower than the iron concentration, magnesium ion vacancies are assumed to be the charge balance defect causing the perturbation.

The double integrated EPR signal intensity is proportional to the concentration of its defect centre at a specific temperature. In the absence of broadening effects the peak-to-peak signal intensity can be used to measure relative concentration. Thus $I_i = a_i X_i$, where I_i is peak-to-peak signal intensity, X_i is the concentration of the defect giving rise to the resonance, and a_i is a proportionality factor dependent on sample size, temperature, peak shape and the instrumental gain of the spectrometer.

3.2. Simple association

According to the equilibrium reaction for dimer formation,

$$Fe_{Mg}^{\cdot} + V_{Mg}'' = D\langle 1\ 1\ 0\rangle,$$

where the dilute solution approximation to the equilibrium constant is given by

$$K_{D\langle 1\,1\,0\rangle} = \frac{[D\langle 1\ 1\ 0\rangle]}{[Fe_{Mg}^{\cdot}]\,[V_{Mg}'']} = K^0_{D\langle 1\,1\,0\rangle} \exp \frac{E_{D\langle 1\,1\,0\rangle}}{k_b T}. \quad (4)$$

Letting

$$I_{Fe_{oct}} = a_{Fe_{oct}}[Fe_{Mg}],$$

$$I_{Fe\langle 1\,1\,0\rangle} = a_{Fe\langle 1\,1\,0\rangle}[D\langle 110\rangle],$$

then

$$\ln \frac{I_{Fe\langle 1\,1\,0\rangle}}{I_{Fe_{oct}}} = \frac{E_{D\langle 1\,1\,0\rangle}}{k_b T} + \ln \frac{a_{Fe_{oct}}[V_{Mg}'']K^0_{D\langle 1\,1\,0\rangle}}{a_{Fe\langle 1\,1\,0\rangle}}. \quad (5)$$

If it is assumed that the ratio $a_{Fe_{oct}}/a_{Fe\langle 1\,1\,0\rangle}$ is constant and that the concentration of vacant magnesium sites is just half the ferric ion concentration at high temperatures and low solute levels where association is slight

$$\ln\left(\frac{a_{Fe_{oct}}[V_{Mg}'']K^0_{D\langle 1\,1\,0\rangle}}{a_{Fe\langle 1\,1\,0\rangle}}\right) = \text{constant at low dopant levels.}$$

Thus, for low dopant level samples at high temperatures a plot of $\ln(I_{Fe\langle 1\,1\,0\rangle}/I_{Fe_{oct}})$ against $1/T$ gives a slope equal to $E_{D\langle 1\,1\,0\rangle}/k_b$, where k_b is Boltzmann's constant.

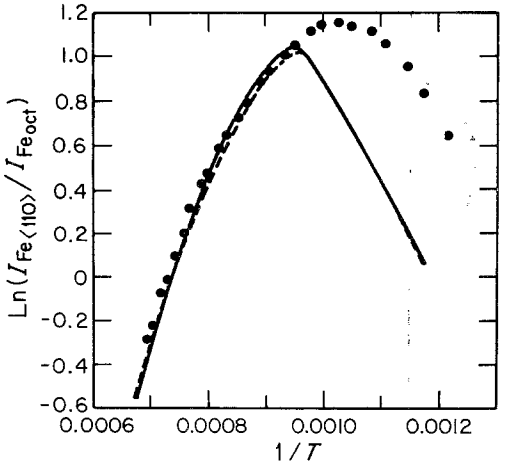

Figure 2 Measured (solid points) and calculated (with [solid line] and without [dashed line] Debye–Hückel corrections) ratios of dimer and isolated iron ion intensities for a sample containing 310 ppm Fe.

Fig. 2 is a plot of Equation 5 in a sample containing 310 ppm Fe. At high temperatures a straight line results, from which the value of $E_{D\langle 1\,1\,0\rangle}$ was calculated to be 0.81 eV. A theoretical value of 0.85 eV for D⟨1 1 0⟩ association was calculated using the HADES shell-model computer program, and a value of 0.65 eV inferred from experimental measurements of oxidation equilibria [1, 2]. This agreement with theory provides evidence for attributing the Fe⟨1 1 0⟩ peak to the dimer. Figs 3 and 4 show similar plots for crystals containing 2300 and 4300 ppm Fe. Since the low solute level approximation is not valid for these samples, more curvature and a lower slope was measured.

The data presented in Figs 2, 3 and 4 were found to be completely reproducible for both increasing and decreasing temperatures and from sample to sample. Similar attempts using the Fe⟨1 0 0⟩ peak gave results which were unreproducible, which suggests that the Fe⟨1 0 0⟩ peak is a sum of several different species. Due to the more complex nature of the Fe⟨1 0 0⟩ peak, it is not used in this study.

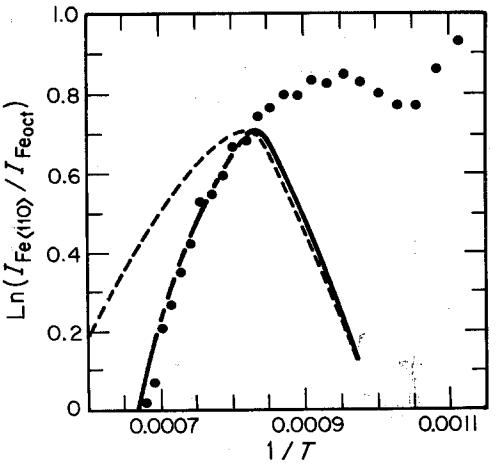

Figure 3 Measured (solid points) and calculated (with [solid line] and without [dashed line] Debye–Hückel corrections) ratios of dimer and isolated iron ion intensities for a sample containing 2300 ppm Fe.

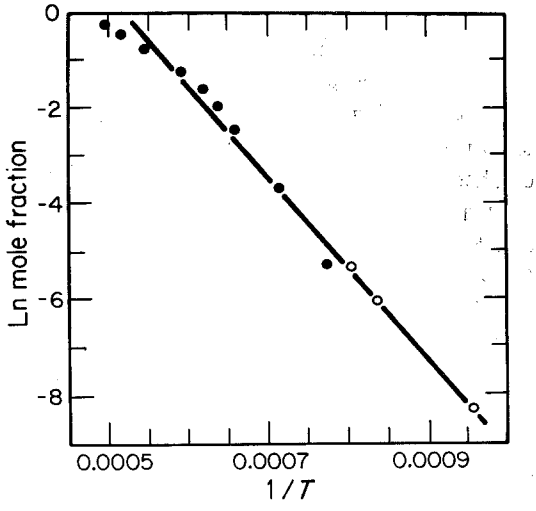

Figure 5 Heat of solution plot for precipitation of $MgFe_2O_4$ from MgO. Solid points are data from Roberts and Merwin [11].

3.3. Phase equilibria

The chemical analyses performed on the 310, 2300 and 4300 ppm Fe-doped samples indicated that the particular samples used actually contained 250, 2340 and 4590 ppm Fe, respectively. Phase separation for these samples was found to occur at 772, 922 and 975° C, respectively. These data, along with the earlier data of Roberts and Merwin [11], are shown in Fig. 5 as a plot of ln (mole fraction on phase boundary) against $1/T$.

4. Discussion

The deviation from a linear relation in Figs 2, 3 and 4 can be attributed to the depletion of vacancies from the system due to association, clustering or precipitation. The extent of association has been estimated by analysing the curvature.

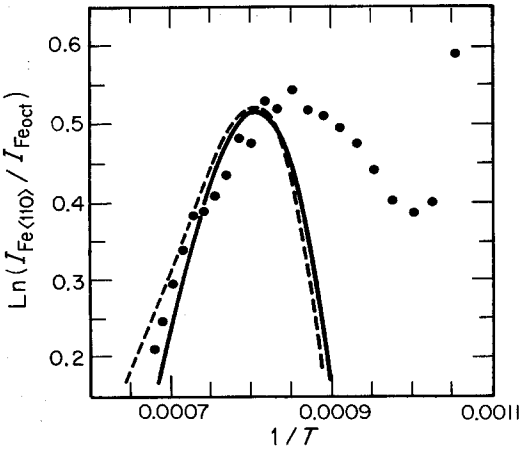

Figure 4 Measured (solid points) and calculated (with [solid line] and without [dashed line] Debye–Hückel corrections) ratios of dimer and isolated iron ion intensities for a sample containing 4300 ppm Fe.

For these rather rough estimations the total iron concentration has been taken to be in the trivalent state, which is too high by 15 to 20% [1, 2] but does not affect any of our conclusions. It is assumed that the total concentration of dimers is proportional to the intensity of the Fe⟨1 1 0⟩ peak and that the equilibrium constant for association can be written

$$\frac{A_{\text{dimer}}}{A_{\text{Fe}_{\text{Mg}}^{\cdot}} A_{\text{V}''_{\text{Mg}}}} = K^0_{\text{D}\langle 1\,1\,0\rangle} \exp \frac{E_{\text{D}\langle 1\,1\,0\rangle}}{k_b T}, \quad (6)$$

where A_i represents the activity of i. Based on the energy for trimer association calculated with a shell model [1, 2], we have the following equilibrium constant for trimer formation

$$\frac{A_{\text{trimer}}}{A_{\text{dimer}} A_{\text{Fe}_{\text{Mg}}^{\cdot}}} = \frac{K^0_{\text{D}\langle 1\,1\,0\rangle}}{24} \exp \frac{1.4\,\text{eV}}{k_b T} \quad (7)$$

where the pre-exponential is taken as the same as for dimer association with an adjustment for configurational entropy. Mass balance equations such as

$$[\text{Fe}_T] = [\text{dimer}] + 2[\text{trimer}] + [\text{Fe}_{\text{Mg}}^{\cdot}] \quad (8)$$

and

$$[\text{V}_T] = 1/2[\text{Fe}_T]$$
$$= [\text{dimer}] + [\text{trimer}] + [\text{V}''_{\text{Mg}}] \quad (9)$$

are incorporated in the analysis, where the sub-

script T indicates total concentration. Using a numerical iterative method with a computer program incorporating Equations 6 to 9, values of $[V''_{Mg}]$ were calculated [3]. If the approximations are valid, the data in Figs 2, 3 and 4 should fit a straight line when $\ln [V''_{Mg}]$ is subtracted from $\ln (I_{Fe\langle 1\,1\,0\rangle}/I_{Fe_{oct}})$ to yield $\ln (I_{Fe\langle 1\,1\,0\rangle}/I_{Fe_{oct}}[V''_{Mg}])$. Initial computations approximated the activity coefficient as unity, where the activity coefficient is defined by

$$f_i = A_i/[i]. \tag{10}$$

Using the data within the one phase temperature region of Fig. 2, $E_{D\langle 1\,1\,0\rangle}$ was first approximated and $K^0_{D\langle 1\,1\,0\rangle}$ was calculated such that Equations 6 to 9 were satisfied. Using linear regression, a best-fit straight line of $\ln (I_{Fe\langle 1\,1\,0\rangle}/I_{Fe_{oct}}[V''_{Mg}])$ against $1/T$ was determined and the regression coefficient, R^2, was calculated. The procedure of picking $E_{D\langle 1\,1\,0\rangle}$ and calculating $K^0_{D\langle 1\,1\,0\rangle}$ was continued to maximize R^2. The equilibrium constant derived was

$$K_{D\langle 1\,1\,0\rangle} = 0.3 \exp\left(\frac{0.85\,\text{eV}}{k_b T}\right) \tag{11}$$

with $R^2 = 0.9995$.

Using the computer program and Equation 11, the values of [dimer] and $[Fe^{\cdot}_{Mg}]$ were calculated to produce a plot of $\ln ([\text{dimer}]/[Fe^{\cdot}_{Mg}])$ against $1/T$ for 310, 2300 and 4300 ppm Fe. Since the ordinate axes in Figs 2, 3 and 4 have only relative (no absolute) meaning, these calculated curves were adjusted in the vertical direction to best fit the data, which gives the dashed lines in these figures. The solid lines in these figures were obtained according to the same procedure, but include Debye–Hückel activity coefficient corrections calculated in a standard way [3, 12, 13]. The corrected equilibrium constant was

$$K_{D\langle 1\,1\,0\rangle} = 0.8 \exp\left(\frac{0.85\,\text{eV}}{k_b T}\right) \tag{12}$$

with $R^2 = 0.9993$. The agreement of these calculated curves over a wide temperature and concentration range is quite good and illustrates the importance of the Debye–Hückel corrections.

A sensitivity analysis of the computer curve-fitting program was conducted to test the limits of suitability. Equations 6 to 9 were adjusted to include additional defects and a range of feasible exponential and pre-exponential values. The range of values found is

$$K_{D\langle 1\,1\,0\rangle} = 0.5 - 2 \exp\left(\frac{0.85 \pm 0.1\,\text{eV}}{k_b T}\right). \tag{13}$$

According to Equation 3, the equilibrium constant for precipitation can be written

$$K_p = \frac{A_{MgFe_2O_4}}{A^2_{Fe^{\cdot}_{Mg}} A_{Mg_{Mg}} A_{V''_{Mg}} A_{O_O}} = K^0_p \exp\left(\frac{E_p}{k_b T}\right). \tag{14}$$

This equation can be simplified by assuming

$$K_p = \frac{1}{(1 - [V''_{Mg}]) f^2_{Fe^{\cdot}_{Mg}} [Fe^{\cdot}_{Mg}]^2 f_{V''_{Mg}} [V''_{Mg}]}. \tag{15}$$

None of these parameters are available experimentally, however, the computer program calculated these values for each concentration at the temperature of phase separation, and Fig. 6 shows a plot of calculated $\ln (K_p)$ values against $1/T$ for the experimental data of Fig. 5. A straight line resulted, yielding a best fit of

$$K_p = 8 \times 10^{-6} \exp \frac{3.8\,\text{eV}}{k_b T}. \tag{16}$$

This equilibrium constant was then incorporated into the computer program and used to calculate the solid curves over the lower temperature range as shown in Figs 2, 3 and 4.

Above the phase separation temperature, an

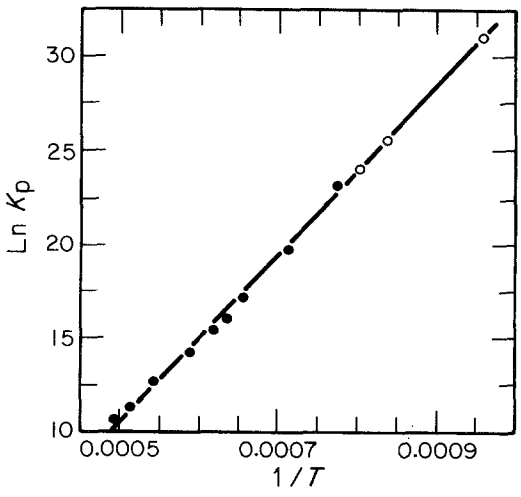

Figure 6 Heat of solution data corrected for defect structure. Solid points are data from Roberts and Merwin [11].

association process with dimer and trimer formation is in satisfactory agreement with experimental data and reasonable assumptions. The derived value of 0.85 eV for the association energy is in reasonable agreement with values of 0.85 eV (calculated) and 0.69 eV (inferred from experimental curve fitting) previously recorded [1, 2] and is not much different from the value of 0.7 eV for scandium-vacancy association inferred from electrical conductivity measurements [14].

Below the phase separation temperature, the calculated ratio of dimers to isolated iron ions consistently lies far below the experimental values, indicating that equilibrium is not achieved. The data indicates that more complex clusters and perhaps mobility limitations control the structure of the crystalline solution, as has been suggested by calculations of cluster stability [1, 2].

Acknowledgement

This research was conducted at the Massachusetts Institute of Technology with the support of the US Department of Energy under Contract No. EY-76-S-02-2390.

References

1. W. H. GOURDIN and W. D. KINGERY, *J. Mater. Sci.* **14** (1979) 2053.
2. W. H. GOURDIN, W. D. KINGERY and J. DRIEAR, *ibid.* **14** (1979) 2074.
3. T. A. YAGER, Ph.D. Thesis, MIT, 1980.
4. T. A. YAGER and W. D. KINGERY, *Rev. Sci. Instrum.* **51** (1980) 464.
5. B. J. WICKS and M. H. LEWIS, *Phys. Stat. Sol. (a)* **6** (1971) 281.
6. S. L. BLANK and J. A. PASK, in "Mass Transport in Oxides", NBS Special Publication Vol. 296, (1968) p. 89.
7. G. P. WIRTZ and M. E. FINE, *J. Appl. Phys.* **38** (1967) 3729.
8. B. HENDERSON, J. E. WERTZ, T. P. P. HALL and R. D. DOWSING, *J. Phys. C.* **4** (1971) 107.
9. R. S. de BIASI and A. CALDAS, *ibid.* **10** (1977) 107.
10. W. LOW, *Proc. Phys. Soc. London* **B69** (1956) 1169.
11. H. S. ROBERTS and H. E. MERWIN, *Amer. J. Sci.* **21** (1931) 145.
12. A. B. LIDIARD, *Phys. Rev.* **94** (1954) 29.
13. E. A. GUGGENHEIM, in "Thermodynamics" (North-Holland Publishing Co., Amsterdam, 1959) Ch.9.
14. D. R. SEMPOLINSKI and W. D. KINGERY, *J. Amer. Ceram. Soc.* **63** (1980) 664.

Received 29 May and accepted 28 July 1980.